Condensation coefficients in plasma sputtering deposition

Pascal Brault §**, Anne-Lise Thomann, Jean-Philippe Rozenbaum**

Groupe de Recherches sur l'Energétique des Milieux Ionisés, UMR6606
CNRS-Université d'Orléans BP 6744, 45067 Orléans Cedex 2, France

Abstract. Optical Emission Spectroscopy and Rutherford Backscattering Spectrometry are combined to determine condensation coefficients for plasma sputtering deposition. The method is applied for palladium deposition onto various substrates and condensation coefficients are found to lie between 0.4 and 0.9.

PACS numbers: 81.15.Cd, 52.77.Dq

Submitted to: *J. Phys. D: Appl. Phys.*

§ Corresponding author: Fax +33(0)2 38 41 71 54, e-mail: `Pascal.Brault@univ-orleans.fr`

Measuring condensation coefficients remains a very difficult task in plasma sputtering deposition. The knowledge of both incoming specie fluxes and deposited amount or growth rates are required in non ideal conditions. Indeed the growing thin film is continuously subjected to ion bombardment and interactions with other energetic species as metastable atoms or molecules, electrons, photons. These species can thus modify the condensation coefficient as compared to vacuum deposition. Thus simple pictures emerging from the description of vacuum deposition can not hold in some situations. Many attempts have been tried, like quartz microbalance, which measures mass differences and thus gives the deposited quantity but alone, it is not sufficient for deducing condensation coefficients. For dielectrics materials or semiconductors ellipsometry can be used for such determination, but it is not appropriate for metals. More sophisticated techniques as laser induced fluorescence and laser or broad band absorption have also been used for evaluating condensation coefficients [1]. In this article we suggest another simple way for the determination of condensation coefficients by combining Optical Emission Spectroscopy (OES) to follow diffusion of depositing species and Rutherford Backscattering Spectrometry (RBS) to measure growth rates for plasma sputtering. The method could be extended to some other plasma deposition methods where the depositing species do not react in the gas phase.

The experimental setup dedicated to plasma sputtering deposition has been widely described elsewhere [2, 3, 4, 5] and is pictured on Fig. 1. Let us recall main features of interest for OES . A low pressure (1-100 mTorr) high frequency (100 MHz) plasma
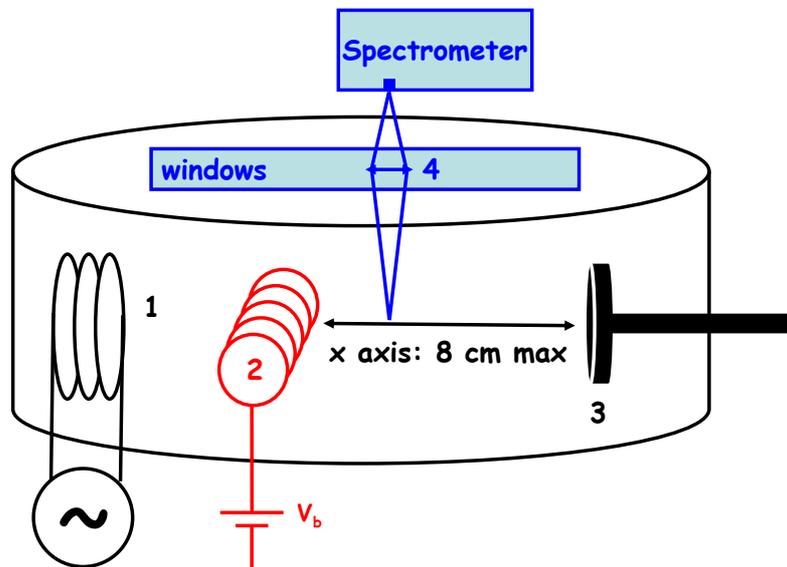

Figure 1. Schematic drawing of the sputtering reactor. 1-High Frequency Antenna creating the plasma, 2- Palladium biased target wire, 3-Grounded substrate, 4-Optical plasma light collection and recording

is created in argon gas with input power of several Watts. The features of this plasma

are reported in Table 1. The metal atom source (an helicoidal wire) is negatively biased

Table 1. Global properties of the sputter plasma [5]. P is the working argon pressure, V_p the plasma potential, V_f the floating potential, n_e the electron density and kT_e the electron temperature at sbstrate position

P (mTorr)	V_p (V)	V_f (V)	n_e (cm^{-3})	kT_e (eV)
100	100	90	5. 10^9	2

($V_b = 0$ to -350 V) so that the plasma ions gain sufficient energy to induce sputtering. Then sputtered atoms travel across the chamber (several cm) and reach the substrate where growth starts. At the same time, the substrate is also exposed to the plasma, and thus submitted during deposition to a ion flux [2, 3]. The substrate temperature is not controlled but was measured to not increase above 310 K. A quartz window is placed on the top of reactor, allowing to collect light emitted by excited Ar and sputtered atoms at various distances from the sputtering wire, with a spatial resolution around 1 mm. Light is collected by an optical fiber connected to the entrance slit of a monochromator (SectraPro 275, Acton Research Corporation). The dispersed light is analysed by a water cooled (-25°C) optical multichannel analyser (EG&G 1453 CCD array) linked to an interface control (EG&G 1471). Data acquisition is monitored by a PC computer through the OMAvision software (EG&G). Growth rates were measured by ex-situ Rutherford Backscattering Spectroscopy using a 2 MeV α particle beam extracted from a Van de Graaf accelerator.

The condensation coefficient $S(x)$ is defined as the ratio of the growth rate to the impinging atom flux :

$$\tau(x) = S(x)\phi(x) \tag{1}$$

where $\phi(x)$ is the impinging atom flux (cm^{-2} s^{-1}) and $\tau(x)$ is the growth rate (cm^{-2} s^{-1}) at the distance x from the sputtering source. $\phi(x)$ can be evaluated using OES in the following way. First, recall that the intensity emitted by atoms excited by an electron impact with mass m_e, energy E, excitation cross-section $\sigma(E)$ and density $n_e(x)$, provided that T_e (the electron temperature), and excited state lifetime are constant over the path length, is given by :

$$I(x) \propto k_e n_e(x) N(x) \tag{2}$$

where $k_e = \int_0^\infty \sigma(E) f(E) \left(\frac{2E}{m_e}\right)^{\frac{1}{2}} dE$ is the excitation rate. k_e is assumed here constant, because in our experiments, we observe that the Ar(750.4 nm) emission line intensity is constant along substrate to target distance x. When it is not the case k_e should depend upon distance x and such dependence should be taken into account. $f(E)$ is the electron energy distribution function, $N(x)$ being the density of atoms in the fundamental state. Thus we have to correlate the intensity $I(x)$ with the atom flux $\phi(x)$ or the density in the fundamental state $N(x)$. It remains only to know the evolution of the electron density $n_e(x)$. If sputter or buffer gas is argon (this is usually the case), such evolution

Table 2. Fitting laws of emission intensities $I_{Pd}(x)$ and growth rates $\tau(x)$ at 100 mTorr.

V_b (V)	$\tau(x)$ (10^{14}cm$^{-2}s^{-1}$)	$I_{Pd}^{363.47nm}(x)$ (arb. units)
-100	$0.4\dfrac{5}{x^2+5}$	$106\dfrac{5}{x^2+5}$
-350	$1.64\dfrac{11}{x^{2.3}+11}$	$289\dfrac{11}{x^{2.3}+11}$

can be determined by recording emission line proportional to $n_e(x)$ as the 750.4 nm line of the 1s^2-2p^1 transition. Indeed, the upper level of this transition is mainly populated by electron collisions from the fundamental level and thus if T_e is constant, then the intensity of this 750.4 nm line becomes proportional to $n_e(x)$. It is also possible to follows $n_e(x)$ evolution from Langmuir probe measurements [4, 5, 6]. In that case,$n_e(x)$is given by the Bohm criterion : $n_e(x) = \dfrac{j(x)}{0.6q}\left(\dfrac{m_i}{kT_e}\right)^{\frac{1}{2}}$ [6] , where $j(x)$ is the measured saturation ion current, m_i being the ion mass, q the elementary electron charge. $\tau(x)$ is measured by RBS on deposits at different distances from the sputtering source. Thus, we have $I(x) \propto N(x)n_e(x)$ and we have also, $\phi(x) \propto N(x)$, when $v(x)$, the velocity of incoming species is constant. Thus $\phi(x) = \alpha\dfrac{I(x)}{n_e(x)}$, where α is a constant and it follows that $\tau(x) = \alpha S(x)\dfrac{I(x)}{n_e(x)}$. Moreover $\phi(x = 0)$ is the flux at the source and in the case of sputtering, it simply reads : $\phi(0) = \dfrac{i\gamma}{qA}$, where i is the target (of area A) current and γ the sputtering yield (which depends on P and V_b). So we can now recover the value of the constant α : $\alpha = \dfrac{i\gamma n_e(0)}{qAI(0)}$ and thus, we find the following simple relation between the condensation coefficient $S(x)$ and the measured quantities $n_e(x)$, $I(x)$ and $\tau(x)$:

$$S(x) = \frac{I(0)}{I(x)}\frac{n_e(x)}{n_e(0)}\frac{qA}{i\gamma}\tau(x) \tag{3}$$

We have used these relations for evaluating the condensation coefficient of sputtered Pd onto SiO$_2$/Si(100). In Figs. 2 and 3 are respectively plotted emission intensities of the Pd 363.47nm line and the Pd growth rates as a fonction of the position in the reactor, for two bias potential values V_b. Both OES and RBS measurements display evolutions that can be expressed in the form : $h(x) = h(0)\dfrac{a}{a+x^n}$. In Table 2 are reported the fitting laws of the emission intensities (363.47 nm line of Pd I) and of growth rates (measured by RBS). Examination of Table 2 shows that n=2 or is closed to 2. The fact that a and n are identical for $\tau(x)$ and $I(x)$ in different conditions results only from the fitting which was not constrained. It means that the sputtered Pd atoms expand spherically in the plasma chamber. This is not surprising because collisions, along the diffusion path, with Ar gas, at 100 mTorr, are sufficient for averaging all the directions. We can also see in Table 2, that $\dfrac{\tau(x)}{I(x)}$ = constant = $\dfrac{\tau(0)}{I(0)}$. Also, in our
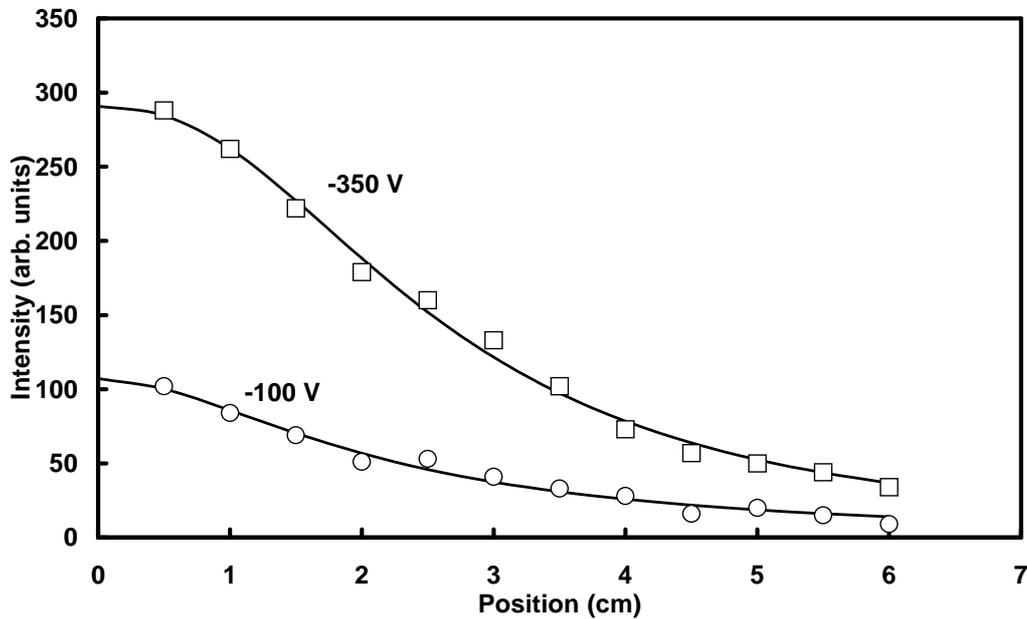
Figure 2. Evolution of the 363.47 nm line of Pd I along the diffusion path between Pd source (x= 0 cm) and the reactor wall. Pressure is 100 mTorr and bias potential is V_b = -100 V (open circle) and V_b = -350 V (open square). The solid lines are the best fits for the diffusion laws (see Table 2)

conditions (P = 100 mTorr), the electron density $n_e(x)$ is constant in the diffusion region [5] then $S(x)$ remains constant along the diffusion path and : $S = \dfrac{qA\tau(0)}{i\gamma}$. We find that the condensation coefficient, at P=100 mTorr, depends on the target bias voltage V_b (and then on pd flux) and takes the value S(Pd/SiO$_2$/Si(100), -100 V) ≈ 0.4 and S(Pd/SiO$_2$/Si(100), -350 V) ≈ 0.85. This can be explained by the fact that, at low Pd incoming flux (i.e. low Pd wire bias voltage), the ratio of Ar ion flux to Pd atoms flux is higher than with larger Pd flux. Thus statistically, deposited Pd atoms suffer more collisions with impinging Ar$^+$ ions, thus Pd desorption during deposition could be increased. So the effective condensation can be lowered. This would be consistent with previous experiments [3] where ions are observed also to increase the compacity of clusters. This could be achieved by desorbing less bound atoms at the periphery of the clusters. Let us examine the values of condensation coefficient on different subtrates. In Table 3 deposited quantities have been measured using RBS on different substrates at P=100mTorr and V_b = -100 V and the estimated condensation coefficient assuming that the deposited quantity ratio between different substrates are the same for condensation coefficient. These condensation coefficients have values close to reported values of Pd for
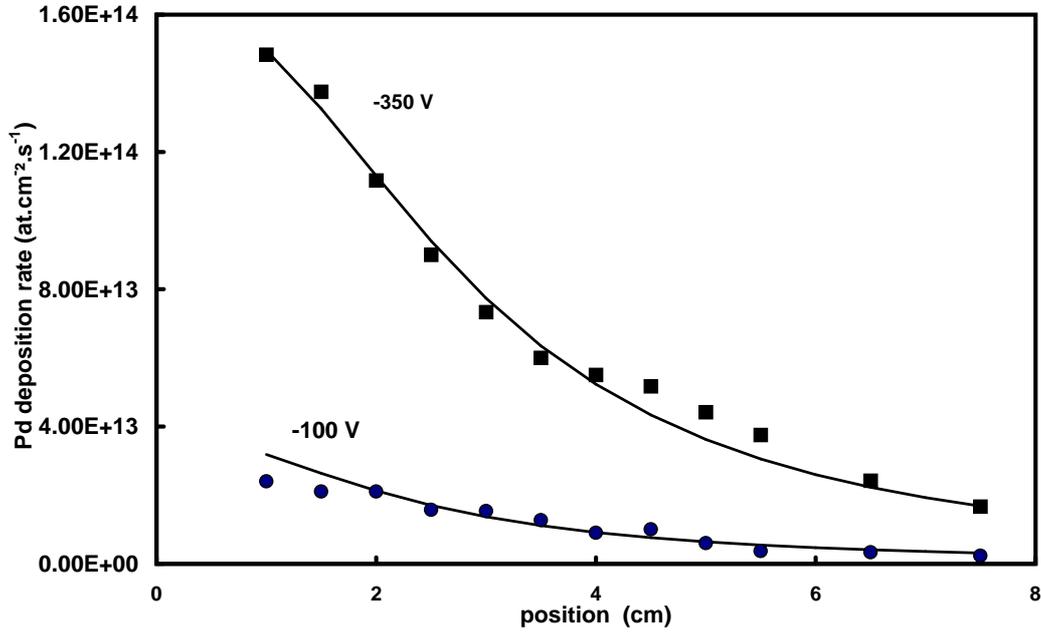
Figure 3. Evolution the Pd growth rate onto SiO_2/Si(100) along the diffusion path between Pd source (x= 0 cm) and and the reactor wall. Pressure is 100 mTorr and Pd target wire bias potential is V_b = -100 V (full circle) and V_b = -350 V (full square). The lines are the best fits for the diffusion laws (see Table 2)

Table 3. Pd condensation coefficients S on various subtrates as deduced from deposited quantities Q and calculated condensation coefficient of Pd on SiO_2/Si(100) at P= 100 mTorr, V_b= -100 V, T=300 K.

Substrate	Q (10^{15}cm^{-2})	S
a-SiO$_2$/Si(100)	2.4	0.4
a-Si$_3$N$_4$/Si(100)	2.4	0.4
a-C/Cu	2.4	0.4
a-Al$_2$O$_3$/Al	3.7	0.6
μc-SiC	5.3	0.9
graphite C(0001)	1.5	0.3

vacuum evaporation on amorphous material as Al_2O_3 where at 300 K, values between 0.7 and 0.9 are reported [7]. Differences originate from different surfaces : highly perturbed surfaces exhibit larger condensation coefficients than smooth surfaces.

In conclusion, a simple way for evaluating condensation coefficients in a plasma environment is proposed by measuring growth rates and recording emission line of the depositing species. A relation giving the condensation coefficient in the case of plasma sputtering is deduced. Condensation coefficients of Pd on various subtrates are thus succesfully estimated.

Acknowledgments

References

[1] Cunge G, Chabert P, Booth J P 2001 *J. Appl. Phys.* **89** 7750 ; Booth J P 1999 *Plasma Sources Sci. Technol.* **8** 249; Sadeghi N, Derouard J and Booth J P 1997 *Plasma Processing of Semiconductors, Proc. of the NATO ASI* (Kluwer Academic Publishers, Dordrecht)
[2] Brault P, Thomann A L, Andreazza-Vignolle C 1998 *Surf. Sci. Lett.* **406** L597
[3] Thomann A L, Rozenbaum J P, Brault P, Andreazza-Vignolle C, Andreazza P 2000 *Appl. Surf. Sci.* **158** 172
[4] Thomann A L, Charles C, Brault P, Laure C and Boswell R 1998 *Plasma Sources Sci. Technol.* **7** 245
[5] Thomann A L, Charles c, Cherradi N and Brault P 2000 *Plasma Sources Sci. Technol.* **9** 176
[6] Grill A *Cold Plasma in Material Fabrications. From Fundamentals to Applications* (IEEE Press, New York, 1994)
[7] Henry C R 1998 *Surf. Sci. Rep.* **31** 231